Long-Range Electron Transfer through a Lipid Monolayer at the Liquid/Liquid Interface

Michael Tsionsky,[†] Allen J. Bard,*,[†] and Michael V. Mirkin*,[‡]

Contribution from the Department of Chemistry and Biochemistry, The University of Texas at Austin, Austin, Texas 78712, and Department of Chemistry and Biochemistry, Queens College−CUNY, Flushing, New York 11367

Abstract: The electron transfer (ET) rate at the interface between two immiscible electrolyte solutions was probed as a function of the driving force and distance between redox centers by scanning electrochemical microscopy. The adsorption of phospholipids at the interface resulted in a decrease in the rate of interfacial ET between aqueous redox species and the oxidized form of zinc porphyrin in benzene. The fraction of the interfacial area covered with lipid (θ) was evaluated from the measured heterogeneous rate constants (k_f). The dependence of θ vs lipid concentration in benzene fit a Langmuir isotherm. For complete monolayers of phospholipids, k_f was a function of the number of methylene groups in a hydrocarbon chain. The driving force dependencies of interfacial ET rates (Tafel plots) were measured for several aqueous redox couples. They were linear, with a transfer coefficient of $\alpha \cong 0.5$ when the driving force for ET ($\Delta G°$) was not too high, in agreement with Marcus theory, and leveled off to the diffusion-controlled rate at larger overpotentials. For even higher $\Delta G°$ and for the first time for heterogeneous ET at a polarizable interface, inverted region behavior was observed.

Introduction

Electron-transfer (ET) reactions are among the most fundamental and thoroughly studied chemical processes.[1] The predictions of Marcus theory have been tested and verified for a number of chemical and biological systems from bimolecular reactions in solutions[2] to intramolecular ET in proteins[3] to electrochemical reactions at metal electrodes modified by self-assembled organic monolayers[4] and at semiconductors.[5] The interface between two immiscible electrolyte solutions (ITIES) is a very interesting intermediate case linking homogeneous and heterogeneous ET. Marcus recently suggested that the classical theory of electron transfer should be applicable to the liquid/liquid interface and proposed expressions for reorganization energy and rate constants.[6] However, the quantitative agreement between the standard rate constants measured at the ITIES and those predicted theoretically has yet to be demonstrated (e.g., see ref 6c). Other authors have argued that the Marcus model may not correctly describe ET at the ITIES.[7]

Experimental studies of ET at the ITIES are scarce,[8−11] and the data are often complicated by coupling of interfacial ET and ion transfer (IT) reactions and experimental artifacts.[12] We have recently demonstrated that many experimental problems can be overcome by using the scanning electrochemical microscope (SECM).[10,13] In these experiments, a tip ultramicroelectrode (UME) with a radius a was placed in an upper liquid phase (e.g., a benzene solution containing the reduced form of zinc porphyrin, ZnPor). The tip was held at a sufficiently positive potential at which ZnPor reacts at the tip surface to produce the oxidized form ZnPor$^+$:

$$ZnPor - e \rightarrow ZnPor^+ \qquad \text{(tip)} \qquad (1)$$

The bottom layer was an aqueous solution of Na$_4$Ru(CN)$_6$. When the tip approached the ITIES (Figure 1A), ZnPor was regenerated at the interface via the bimolecular redox reaction

$$ZnPor^+ + Ru(CN)_6{}^{4-} \xrightarrow{k_f} ZnPor + Ru(CN)_6{}^{3-} \qquad \text{(ITIES)}$$
$$(2)$$
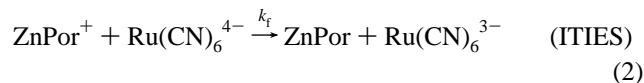
[†] The University of Texas at Austin.

[‡] Queens College−CUNY.

[⊗] Abstract published in *Advance ACS Abstracts,* October 15, 1997.

(1) (a) Marcus, R. A.; Sutin, N. *Biochim. Biophys. Acta* **1985**, *811*, 265. (b) Barbara, P. F.; Meyer, T. J.; Ratner, M. A. *J. Phys. Chem.* **1996**, *100*, 13148.

(2) Miller, J. R.; Calcaterra, L. T.; Closs, G. L. *J. Am. Chem. Soc.* **1984**, *106*, 3047.

(3) (a) Winkler, J. R.; Gray, H. B. *Chem. Rev.* **1992**, *92*, 369. (b) McLendon, G.; Hake, R. *Chem. Rev.* **1992**, *92*, 481.

(4) (a) Chidsey, C. E. D. *Science* **1991**, *251*, 919. (b) Finklea, H. O. In *Electroanalytical Chemistry*; Bard, A. J., Ed.; Marcel Dekker: New York, 1996; Vol. 19, p 109. (c) Miller, C. J. In *Physical Electrochemistry: Principles, Methods, and Applications*; Rubinstein, I., Ed.; Marcel Dekker: New York, 1995; p 27.

(5) Lu, H.; Prieskorn, J. N.; Hupp, J. T. *J. Am. Chem. Soc.* **1993**, *115*, 4927.

(6) (a) Marcus, R. A. *J. Phys. Chem.* **1990**, *94*, 1050. (b) Marcus, R. A. *J. Phys. Chem.* **1990**, *94*, 4152; addendum, *J. Phys. Chem.* **1990**, *94*, 7742. (c) Marcus, R. A. *J. Phys. Chem.* **1991,** *95*, 2010; addendum, *J. Phys. Chem.* **1995**, *99*, 5742.

(7) Smith, B. B.; Halley, J. W.; Nozik, A. *J. Chem. Phys.* **1996**, *205*, 245.

(8) Samec, Z.; Marecek, V.; Weber, J.; Homolka, D. *J. Electroanal. Chem.* **1981**, *126*, 105.

(9) (a) Geblewicz, G.; Schiffrin, D. J. *J. Electroanal. Chem.* **1988**, *244*, 27. (b) Cunnane, V. J.; Schiffrin, D. J.; Beltran, C.; Geblewicz, G.; Solomon, T. *J. Electroanal. Chem.* **1988**, *247*, 203. (c) Cheng, Y.; Schiffrin, D. J. *J. Electroanal. Chem.* **1991**, *314,* 153. (d) Cheng, Y.; Schiffrin, D. J. *J. Chem. Soc., Faraday Trans.* **1993**, *89*, 199.

(10) Wei, C.; Bard, A. J.; Mirkin, M. V. *J. Phys. Chem.* **1995**, *99*, 16033.

(11) Nakatani, K.; Chikama, K.; Kitamura, N. *Chem. Phys. Lett.* **1995**, *237*, 133.

(12) (a) Girault, H. H.; Schiffrin, D. J. In *Electroanalytical Chemistry*; Bard, A. J., Ed.; Marcel Dekker: New York, 1989; Vol. 15, p 1. (b) Senda, M.; Kakiuchi, T.; Osakai, T. *Electrochim. Acta* **1991**, *36*, 253. (c) Girault, H. H. In *Modern Aspects of Electrochemistry*; Bockris, J. O'M., Conway, B. E., White, R. E., Eds.; Plenum Press: New York, 1993; Vol. 25, p 1. (d) Samec, Z.; Kakiuchi, T. In *Advances in Electrochemical Science and Electrochemical Engineering*; Gerischer, H., Tobias, C. W., Eds.; VCH: New York, 1995; Vol. 4, p 297. (e) Benjamin, I. *Chem. Rev.* **1996**, *96*, 1449. (f) Eisenthal, K. B. *Chem. Rev.* **1996**, *96*, 1343.

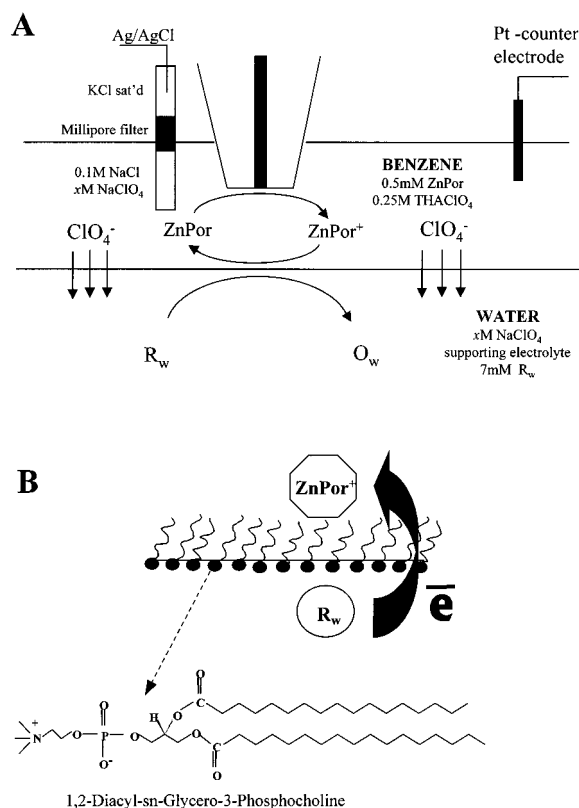(13) Tsionsky, M.; Bard, A. J.; Mirkin, M. V. *J. Phys. Chem.* **1996**, *100*, 17881.

A

B

1,2-Diacyl-sn-Glycero-3-Phosphocholine

Figure 1. (A) Probing the kinetics of ET between $ZnPor^+$ and various aqueous redox species at the ITIES with the SECM. The SECM was operated in the conventional feedback mode. O_w and R_w represent one of the following aqueous redox couples: $Ru(CN)_6^{3/4-}$, $Mo(CN)_8^{3/4-}$, $Fe(CN)_6^{3/4-}$, $Fe^{3/2+}$, $V^{3/2+}$, or Co(III)/(II) sepalchrate. Of the ionic species contained in the system, only ClO_4^- can readily cross the interface to maintain electroneutrality. (B) The ITIES modified by a monolayer of phospholipid. The inset shows the structure of synthetic phosphatidyl choline lipids.

and the tip current (i_T) increased with a decrease in the tip−ITIES separation, d, (positive feedback). If no regeneration of ZnPor occurs (e.g., with no $Ru(CN)_6^{4-}$ species in the bottom layer), the ITIES only blocks mediator diffusion to the tip, so i_T decreases at smaller d (negative feedback). In this experiment the UME tip probes the interface directly, allowing quantitative separation of ET from IT.[10,13]

While conventional studies of the ITIES have been carried out at externally biased ITIES, in SECM measurements the potential across the interface is adjusted by varying the concentration of a common ion (e.g., ClO_4^-) in the two liquid phases, providing a controllable driving force for charge-transfer reactions. The interfacial potential drop in V, $\Delta_w^o\varphi$, is governed by the ratio of the common ion concentration in water, $[ClO_4^-]_w$, and the organic phase, $[ClO_4^-]_o$. In our experiments $[ClO_4^-]_o$ was kept constant, and the relative values of the potential drop across the ITIES, assuming unity activity coefficients, can be expressed as

$$\Delta_w^o\varphi = \text{const} - 0.06 \log [ClO_4^-]_w \qquad (3)$$

The effective heterogeneous rate constant (k_f) of reaction 2 evaluated from the tip current−distance (i_T−d) curves was directly proportional to the concentration of $Ru(CN)_6^{4-}$ in the aqueous solution, and the log k_f vs $\Delta_w^o\varphi$ dependence (Tafel plot) was linear with a transfer coefficient of $\alpha = 0.5$.[13] This was the first demonstration that conventional ET theory (a Butler−Volmer model) is applicable to the liquid/liquid interface when the driving force is not too high.

The experiments described below are aimed at testing the two most important predictions of ET theory at the liquid/liquid interface, i.e., exponential decrease of the ET rate with increasing distance between two redox moieties and quadratic dependence of activation energy vs driving force. The latter should result in the well-known Marcus inverted region behavior at large overpotentials. Both effects can be investigated using a molecular monolayer as a spacer between the electron donor and acceptor (Figure 1B). This approach has been used to study ET processes at solid electrodes,[4] but not previously for kinetic measurements at the ITIES. It is, in fact, much easier to form an organized molecular monolayer on the ITIES than on the solid/liquid interface, since no specific chemical interaction between the substrate and adsorbate (like thiol/Au)[4] is required. Unlike solid electrodes, the ITIES is atomically smooth and highly uniform, so the common problems of surface defects and pinholes in the monolayer are absent. Saturated symmetric phospholipids were employed as a spacer in this study. They have been shown previously to adsorb readily and form stable, compact monolayers at both water/air and water/organic interfaces.[14] Charge-transfer processes at the lipid-modified ITIES are also relevant to those at biological membranes.[15]

Another objective of this work is to use ET as a yardstick to probe structures and physicochemical properties of complicated systems. For example, the well-established exponential distance dependence of the rate of ET has been used to evaluate conductivity of DNA strands by measuring the tunneling parameter, β_r.[16] Groves and co-workers used a somewhat similar approach to characterize multiheme molecular ensembles in phospholipid vesicles.[17] The possibility of extracting microscopic information about ITIES from kinetic data would also be useful, because details about the interfacial structure remain sparse, in spite of several decades of active studies.[12] For example, from the previously measured α value of 0.5 we inferred that the participants of the ET reaction are separated by a thin interfacial boundary (which they cannot significantly penetrate) rather than reside in a mixed, fairly thick, interfacial layer (in which case, the potential drop between two redox molecules would be much smaller than the total $\Delta_w^o\varphi$ and α would be $<<0.5$).[13] This observation is consistent with the sharp interface model[6a] or with the assumption of an angstrom thick, ion-free layer at the interface separating participants of the redox reaction.[18] In this paper, we investigate the structure of a lipid monolayer adsorbed at the ITIES from the distance dependence of the ET rate.

Experimental Section

Chemicals. 5,10,15,20-Tetraphenyl-21H,23H-porphine Zn (ZnPor) from Aldrich (Milwaukee, WI) and benzene (J. T. Baker Inc., Phillisburg, NJ) were used as received. Tetrahexylammonium perchlorate (THAClO$_4$; Fluka Chemika, Switzerland) was recrystallized twice from an ethyl acetate:ether (9:1) mixture and dried under vacuum

(14) (a) Larsson, K.; Quinn P. J. In *The Lipid Handbook*; Gunstone, F. D., Harwood, J. L., Padley, F. B., Eds.; Chapman & Hall: London, 1994; p 401. (b) Girault, H. H.; Schiffrin, D. J. *J. Electroanal. Chem.* **1984**, *179*, 277. (c) Kakiuchi, T.; Yamane, M.; Osakai, T.; Senda, M. *Bull. Chem. Soc. Jpn.* **1987**, *60*, 4223.

(15) (a) Girault, H. H.; Schiffrin, D. J. In *Charge and Field Effects in Biosystems*; Allen, M. J., Usherwood, P. N. R., Eds.; Abacus Press: Turnbridge Wells, England, 1984; p 171. (b) Ohkouchi, T.; Kakutani, T.; Senda, M. *Bioelectrochem. Bioenerg.* **1991**, *25*, 81. (c) Gennis, R. B. *Biomembranes*; Springer: New York, 1995. (d) Shirai, O.; Yoshida, Y.; Matsui, M.; Maeda, K.; Kihara, S. *Bull. Chem. Soc. Jpn.* **1996**, *69*, 1.

(16) (a) Murphy, C. J.; Arkin, M. R.; Jenkins, Y.; Barton, J. K. *Science* **1993**, *262*, 1025. (b) Brun, A. M.; Harriman, A. *J. Am. Chem. Soc.* **1992**, *114*, 3656.

(17) Lahiri, J.; Fate, G. D.; Ungashe, S. B.; Groves, J. T. *J. Am. Chem. Soc.* **1996**, *118*, 2347.

(18) Kakiuchi, T.; Senda, M. *Bull. Chem. Soc. Jpn.* **1983**, *56*, 1753.

overnight at room temperature. Before measurements, a benzene solution containing 0.25 M THAClO$_4$ and 0.5 mM ZnPor was mixed with at least a twice larger volume of water by vigorous shaking to produce a water/benzene emulsion. This emulsion was centrifuged to separate the benzene solution from the aqueous phase. This procedure was repeated twice to remove trace amounts of surfactants from the organic phase that might adsorb on the benzene/water interface.

Chloroform solutions of symmetric saturated synthetic lipids (1,2-dicacyl-*sn*-glycero-3-phosphocholine) with different numbers of methylene groups in a hydrocarbon chain (n = 10, 12, 14, 16, 18, 20; the abbreviations C-10, C-12, etc., will be used to designate different phospholipids) from Avanti Polar Lipids, Inc. (Alabaster, AL) were stored at −20 °C. Before an experiment, a flow of nitrogen was passed above a small volume (∼40 μL) of phospolipid solution in chloroform for complete evaporation of solvent. The precipitated lipid was then redissolved in benzene to prepare a 500 μM stock solution, which also contained 0.5 mM ZnPor and 0.25 M THAClO$_4$. Heating to 50−60 °C for 3−5 min was required to obtain high concentrations of the larger lipids (C-18 and C-20) in benzene. The mixture of the lipid stock solution and benzene solution containing the same concentrations of ZnPor and THAClO$_4$ served as the organic phase.

Aqueous solutions were prepared from NaClO$_4$, NaCl, H$_2$SO$_4$, and FeSO$_4$ (Johnson Matthey, Ward Hill, MA). Na$_4$Ru(CN)$_6$ and Na$_4$Mo(CN)$_8$ were synthesized by methods proposed earlier for K$_4$Ru(CN)$_6$[19] and K$_4$Mo(CN)$_8$,[20] where NaOH and NaCN were used instead of KOH and KCN. Na$_4$Ru(CN)$_6$ and Na$_4$Mo(CN)$_8$ were recrystallized several times from methanol:water and dried under vacuum overnight at 50 °C. Solutions of V(II) or Co(II) sepalchrate were prepared by bulk electrolysis of VCl$_3$ (Aldrich) or Co(III) sepalchrate (Aldrich), respectively, at a Hg-pool cathode under a nitrogen atmosphere. The electrolysis was considered complete when the current decreased to 1% of the initial value (usually 3−5 h). All aqueous solutions were prepared from deionized water (Milli-Q, Millipore Corp.).

Electrodes and Electrochemical Cells. Pt wires (25-μm diameter, Goodfellow, Cambridge, U.K.) were heat-sealed in glass capillaries to prepare SECM tips as described previously.[21] The tip electrode was rinsed with ethanol and water and then polished and dried before each measurement. A three-electrode configuration was used in all experiments, and all electrodes were placed in the top (organic) phase. The SECM cell was described previously.[13] An ionic bridge containing a solution of NaCl and NaClO$_4$ was placed between the Ag/AgCl reference electrode and benzene solution. To measure the ET rates, the top phase contained a solution of 0.25 M THAClO$_4$, 0.5 mM ZnPor, and 0−100 μM lipid in benzene, and the bottom phase contained a solution of 0.1 M NaCl, 0.01−2 M NaClO$_4$, and 7 mM of Na$_4$Ru(CN)$_6$ or other oxidizable aqueous species (i.e., Na$_4$Fe(CN)$_6$, Na$_4$Mo(CN)$_8$, VCl$_2$, FeSO$_4$, or Co(II) sepalchrate chloride). The benzene solution was deaerated before each experiment. The experiments with V(II) and Co(II) sepalchrate were carried out in a glovebag under nitrogen. A 0.5 M H$_2$SO$_4$ solution was used as a supporting electrolyte instead of 0.1 M NaCl to avoid extraction of chloride complexes into the organic phase.

SECM Apparatus and Procedure. The SECM instrument has been described previously.[22] Before SECM measurements, the 25-μm tip electrode was positioned in the top (benzene) phase. A typical steady-state voltammogram of ZnPor obtained at the tip in a benzene solution (Figure 2A) consists of two well-defined waves corresponding to two one-electron oxidations of ZnPor to ZnPor$^+$ and ZnPor^{2+}. In all SECM experiments the tip was biased at a potential corresponding to the plateau current of the first oxidation wave of ZnPor. A comparison of cyclic voltammograms in Figure 2A,B shows that the tip process was unaffected by the presence of micromolar concentrations of lipid in benzene.

The approach curves were obtained by moving the tip toward the liquid/liquid interface and recording i_T as a function of d. The coordinate of the ITIES (d = 0) was determined from the sharp increase

(19) Krause, R. A.; Violette, C. *Inorg. Chim. Acta* **1986**, *113*, 161.
(20) Furman, N. H.; Miller, C. O. In *Inorganic Syntheses*; Andrieth, L. F., Ed.; McGraw-Hill: New York, 1950; Vol. III, p 160.
(21) Bard, A. J.; Fan, F.-R. F.; Kwak, J.; Lev, O. *Anal. Chem.* **1989**, *61*, 1794.
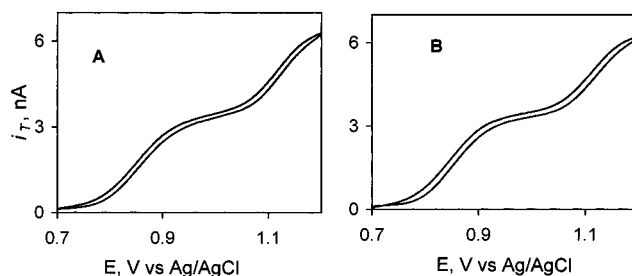(22) Wipf, D. O.; Bard, A. J. *J. Electrochem. Soc.* **1991**, *138*, 489.

Figure 2. Steady-state voltammograms of ZnPor in benzene at a 25-μm diameter Pt microdisk. Scan rate, 25 mV/s. (A) 1 mM ZnPor and 0.25 M THAClO$_4$; (B) 1 mM ZnPor, 0.25 M THAClO$_4$, and 100 μM C-10 lipid.

(or decrease, if the bottom phase contained no redox species) in i_T that occurred when the tip touched the ITIES.

Results and Discussion

Driving Force Dependence of the ET Rate at a Lipid-Free Interface. Our recent study demonstrated that the effective heterogeneous rate constant of the ET reaction (eq 2) at the water/benzene interface is an exponential function of $\Delta_w^o \varphi$ (eq 3).[13] This finding was consistent with the linear driving force dependence of activation energy expected at low overpotentials[6,9]

$$\Delta G^{\ddagger} = \alpha \Delta G^{\circ} \qquad (4)$$

where $\Delta G^{\ddagger}$ is the free energy barrier (J/mol) and α (∼0.5) is the transfer coefficient. However, the driving force for the interfacial ET reaction should include not only the $\Delta_w^o \varphi$ term but also the difference of standard potentials of the organic and aqueous redox mediators:

$$\Delta G^{\circ} = -F(\Delta E^{\circ} + \Delta_w^o \varphi) \qquad (5)$$

To investigate the dependence of k_f on ΔE°, we obtained i_T−d curves for ET reactions between ZnPor$^+$ and different aqueous complex ions R$_w$ (where R$_w$ = Ru(CN)$_6^{4-}$, Mo(CN)$_8^{4-}$, Fe(CN)$_6^{4-}$, and V(II) or Co(II) sepalchrate):

$$\text{ZnPor}^+ + \text{R}_w \rightarrow \text{ZnPor} + \text{O}_w \qquad \text{(at the ITIES)} \quad (6)$$
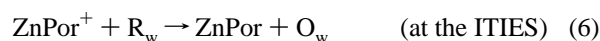
Neither form of the aqueous redox couple (R$_w$/O$_w$) has appreciable solubility in benzene, and as discussed previously,[13] both ZnPor and ZnPor$^+$ remain in the benzene phase. Because of benzene's low dielectric constant, the ZnPor$^+$ probably exists predominantly as ion pairs with ClO$_4^-$; these are represented in this paper by ZnPor$^+$. The NaClO$_4$ concentration in benzene was maintained high and constant throughout all of the experiments (0.25 M), so the same species participated in the ET reaction.

The ET reaction (eq 6) injects positive charge into the aqueous phase which is compensated by the IT of the common ClO$_4^-$ ion from benzene to water. At low concentrations of the common ion (e.g., less than 10 mM), the IT may become the rate-determining step.[10] To avoid this complication, the concentration of ClO$_4^-$ in benzene was kept high (0.25 M) in all experiments. This also helped to decrease the ohmic potential drop in the highly resistive benzene solution. To eliminate the possible complication of slow diffusion of redox species in the aqueous phase, the concentration of the aqueous redox mediator was always 14 times higher than the ZnPor concentration in benzene. Under these conditions, the effective heterogeneous rate constant for the ET reaction (eq 2) can be extracted from the i_T vs d curve using the previously developed theory.[10,13]
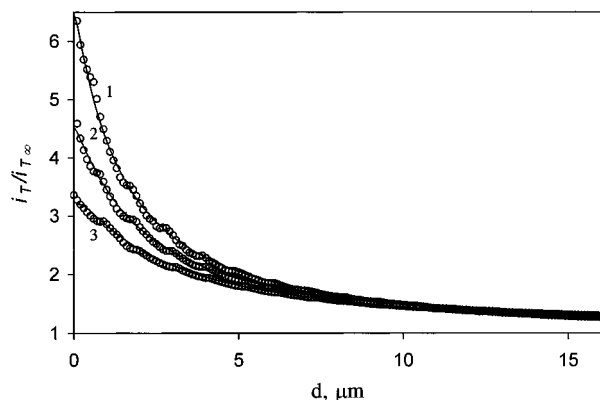
Figure 3. Current vs distance curves for a 25-μm Pt tip approaching water from a benzene solution containing 0.5 mM ZnPor and 0.25 M THAClO$_4$. The aqueous phase contained 0.1 M NaCl, 0.1 M NaClO$_4$, and 7 mM of (1) Fe(CN)$_6^{4-}$, (2) Mo(CN)$_8^{4-}$, and (3) Ru(CN)$_6^{4-}$. The same value of $\Delta_w^o\varphi$ for all curves was determined by the constant ratio of perchlorate concentrations in the two phases. The tip was scanned at 1 μm/s.
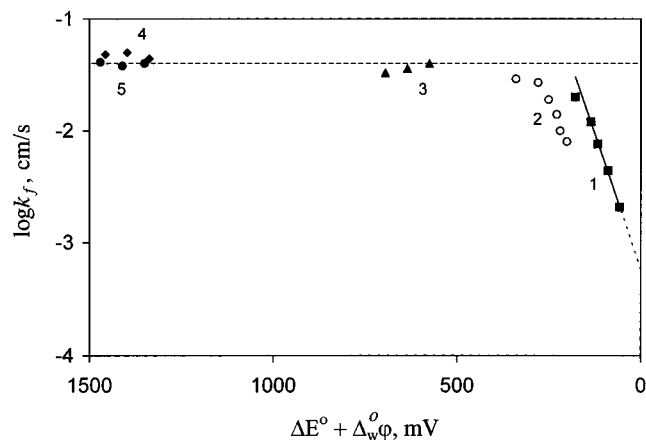

Figure 4. Potential dependence of the rate of ET between ZnPor$^+$ and various aqueous redox species. The abscissa plots the driving force for ET given by eq 7. The aqueous solution contained 0.01$-$2 M NaClO$_4$ and 7 mM of (1) Ru(CN)$_6^{4-}$, (2) Mo(CN)$_8^{4-}$, (3) Fe(CN)$_6^{4-}$, (4) Co(II) sepalchrate, and (5) V^{2+}. The aqueous supporting electrolyte was (1$-$4) 0.1 M NaCl and (5) 0.5 M H$_2$SO$_4$. For other parameters, see Figure 3. Horizontal dashed line shows the diffusion limit for the ET rate measurements by SECM with a 25-μm tip ($\sim$0.03 cm/s). The rate constants are calculated using the diffusion coefficient of ZnPor, $D = 4 \times 10^{-6}$ cm^2/s.

Three i_T vs d curves obtained for ET reactions between ZnPor$^+$ and Ru(CN)$_6^{4-}$, Mo(CN)$_8^{4-}$, and Fe(CN)$_6^{4-}$ at the same $\Delta_w^o\varphi$ are shown in Figure 3. To enable comparison with the theory, the measured current was always normalized by the tip current at an infinite tip-substrate separation, $i_{T,\infty}$. Assuming that standard rate constants (i.e., k_f at $\Delta G^\circ = 0$) are similar, the differences in ET rates for these reactants may only be due to the different ΔE° values. The formal potentials for Ru(CN)$_6^{3/4-}$, Mo(CN)$_8^{3/4-}$, and Fe(CN)$_6^{3/4-}$ couples measured by cyclic voltammetry are 750, 590, and 235 mV vs Ag/AgCl, respectively. Accordingly, curve 2 in Figure 3, corresponding to Mo(CN)$_8^{4-}$, shows a higher feedback current than curve 3 obtained with Ru(CN)$_6^{4-}$ in water. With Fe(CN)$_6^{4-}$, the ET rate is much higher, and the overall process is diffusion controlled (curve 1).

More quantitatively, one can compare potential dependencies of k_f (Tafel plots) obtained for the different redox species (Figure 4). Values of k_f were obtained by the best fit (lines on Figure 3) of experimental results (circles on Figure 3) using eq 12 of

ref 10. The uncertainty in such calculations of k_f does not exceed 5%. The driving force for interfacial ET is given by $\Delta E^\circ + \Delta_w^o\varphi$. Since the diffusion coefficients of oxidized and reduced forms should be similar for all redox couples of interest, we assumed the formal potentials to be equal to reversible half-wave potentials ($E_{1/2}$). For aqueous redox couples, these values were found from cyclic voltammetry vs an aqueous reference electrode. The E° value for ZnPor$^{+/0}$ was evaluated as a half-wave potential of the nernstian steady-state voltammogram obtained at a 7-μm carbon microelectrode. As the $E_{1/2}$ values for both the aqueous redox species and ZnPor in benzene were measured with respect to the same aqueous reference electrode, the difference of these values is

$$E_{1/2} \cong \Delta E^\circ + \Delta_w^o\varphi \qquad (7)$$

Although the absolute value of $\Delta_w^o\varphi$ cannot be found without an extrathermodynamic assumption,[12] $\Delta E_{1/2}$ gives the absolute value of the driving force, according to eq 5.

For Ru(CN)$_6^{4-}$ and Mo(CN)$_8^{4-}$, the Tafel plots in Figure 4 are linear and the transfer coefficients obtained from their slopes are very close to 0.5. The horizontal shift between these two straight lines corresponds to the $\sim$150 mV difference between the formal potentials of the Ru(CN)$_6^{3/4-}$ and Mo(CN)$_8^{3/4-}$ redox couples. For Mo(CN)$_8^{4-}$, the Tafel plot leveled off at higher overpotentials as k_f approached the diffusion limit (i.e., about 0.035 cm/s, corresponding to the rate of diffusion of ZnPor$^+$ in the gap between the tip and the ITIES). The k_f for ET between Fe(CN)$_6^{4-}$ and ZnPor$^+$ was above the diffusion limit at any $\Delta_w^o\varphi$ value in Figure 4. The same diffusion limit can be seen for two more negative aqueous redox species, V^{2+} and Co(II) sepalchrate.

The extrapolation of the linear Tafel plot obtained with Ru(CN)$_6^{4-}$ to zero driving force gives the effective heterogeneous rate constant, $k^\circ = 5.88 \times 10^{-4}$ cm/s. This corresponds to the bimolecular rate constant, $k_{12} = k^\circ/[\text{Ru(CN)}_6^{4-}] = 0.084$ M^{-1} cm s^{-1}, which is close to the value of k_{12} obtained at the water/nitrobenzene interface for ET between Fc and FcCOO$^-$ (0.06 M^{-1} cm s^{-1}).[10] A more quantitative comparison between this value and the Marcus theory prediction is difficult because of the lack of literature data on either electrochemical rate constants or homogeneous self-exchange rates for the Ru(CN)$_6^{3/4-}$ and ZnPor$^{+/0}$ couples.

The demonstrated dependencies of k_f on both ΔE° and $\Delta_w^o\varphi$ allow us to exclude the possibility that the measured kinetics relate to an IT rather than an ET reaction.[12c] For instance, one can assume that ZnPor$^+$ first crosses the interface, and this IT process is followed by homogeneous ET. In this scheme, the apparent dependence of the overall rate on $\Delta_w^o\varphi$ can be ascribed to the IT reaction. However, if the transfer of ZnPor$^+$ were rate-limiting, k_f should be independent of ΔE°. If, on the other hand, homogeneous ET were the slow step, the overall rate would be independent of $\Delta_w^o\varphi$.

Reversible Adsorption of Phospholipids at the Interface. Amphiphilic molecules like lipids dissolved in an organic phase spontaneously form a monolayer film at the water/organic interface. The orientation of the monolayer is such that the hydrophilic head group is immersed in water, while the hydrophobic tail remains in the organic phase. An attempt to probe ET across a phospholipid monolayer adsorbed at the ITIES was reported recently by Cheng and Schiffrin, who found that a monolayer makes ET immeasurably slow.[23] Our measurements also showed a strong blocking effect of adsorbed lipids

(23) Cheng, Y.; Schiffrin, D. J. *J. Chem. Soc., Faraday Trans.* **1994**, *90,* 2517.
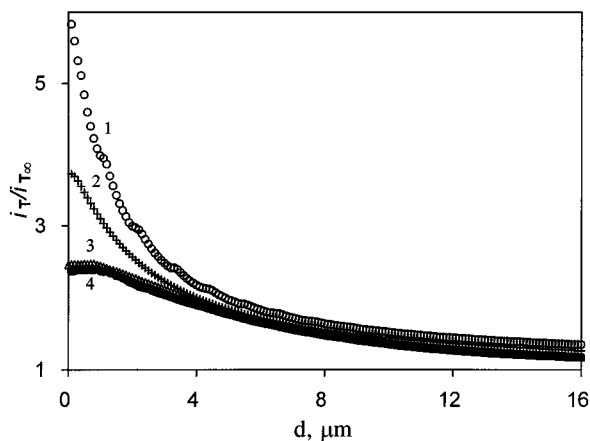
Figure 5. Time dependence of lipid adsorption on the ITIES for a 25-μm Pt UME in benzene approaching the water/benzene interface. The aqueous solution contained 0.1 M NaCl, 0.1 M NaClO$_4$, and 7 mM Na$_4$Fe(CN)$_6$. $i_{T,\infty}$ = 0.95 nA. For other parameters, see Figure 3. Curve 1 was recorded immediately after lipid injection, other curves were obtained (2) 5, (3) 28, and (4) 50 min after injection of 15.8 μM C-10 lipid into the organic phase.
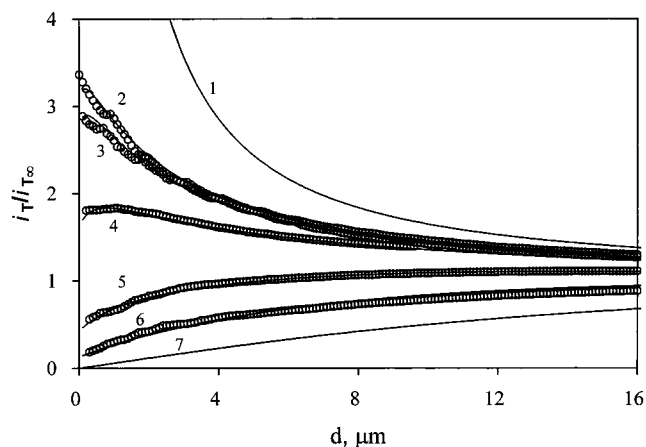

Figure 6. Effect of lipid concentration on the shape of the SECM current−distance curves. The aqueous solution was 0.1 M NaCl, 0.1 M NaClO$_4$, and 7 mM Na$_4$Ru(CN)$_6$. The concentration of C-10 lipid in benzene was (2) 0, (3) 1.12, (4) 3.54, (5) 12.4, and (6) 47.8 μM. Circles are experimental points. Solid lines represent the theory for the following k_f values (cm/s): (1) ∞ (diffusion-controlled process), (2) 0.0145, (3) 0.013, (4) 0.0075, (5) 0.002, (6) 0.0006, and (7) 0 (pure negative feedback). The tip was scanned at 1 μm/s.
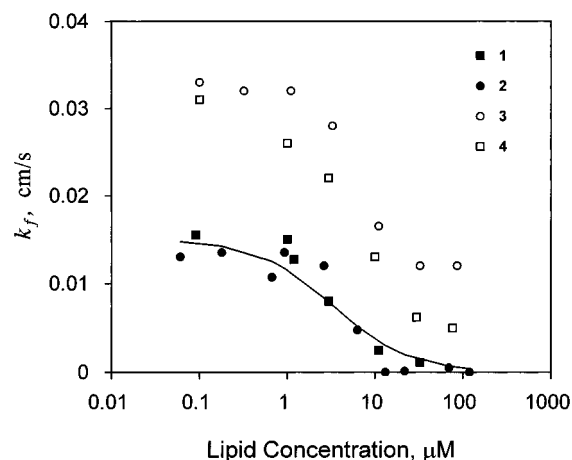

Figure 7. Dependence of the rate constant of ET between ZnPor$^+$ and Ru(CN)$_6$$^{4-}$ (■ and ●) or Fe(CN)$_6$$^{4-}$ (○ and □) on lipid concentration in benzene. The number of methylene groups in the lipid hydrocarbon chain was: 10 (■ and ○), 12 (□), and 20 (●). The organic phase contained 0.25 M THAClO$_4$, 0.5 mM ZnPor, and lipid. The water phase contained 0.1 M NaCl, 0.1 M NaClO$_4$, and 7 mM Ru(CN)$_6$$^{4-}$ (■ and ●) or Fe(CN)$_6$$^{4-}$ (○ and □). Rate constants were obtained by fitting experimental approach curves (Figure 6) to the theory.[10,13] The solid line represents the Frumkin isotherm (eq 11) with B = 2 × 10^5 M^{-1} and a = 0.25.

on interfacial ET. Figure 5 represents the time dependence of current−distance curves for ET between Fe(CN)$_6$$^{4-}$ and ZnPor$^+$ obtained after addition of a lipid stock solution to the organic phase to produce a 27 μM solution of C-10 in benzene. Immediately after the addition, when the coverage of the ITIES with lipid was negligible, the ET reaction was diffusion-controlled (curve 1). After 5 min, a significant decrease in feedback current (curve 2) indicates that lipid molecules have covered a large fraction of the ITIES area during this period. The blocking effect further increased after 28 min (curve 3). There was, however, no appreciable difference between the approach curves obtained after 28 and 50 min (curve 4). The results in Figure 5 suggest that adsorption of lipid molecules on the ITIES is a diffusion-controlled process,[24] which comes to equilibrium within 30−40 min.

The blocking effect of a lipid film can be attributed to the decrease in either the ET or IT rate. However, Kakiuchi and co-workers and Schiffrin and co-workers[25] extensively studied the effect of different lipid monolayers on the rate of ion transfer of various ions, including ClO$_4$$^-$. The largest decrease in the IT rate caused by the presence of a compact phospholipid monolayer at the ITIES was by a factor of 5. The effects observed here are orders of magnitude larger. With a 0.25 M concentration of THAClO$_4$ in benzene, the IT rate would have had to decrease by at least by a factor of 100−1000 to account for the effects observed. It was also shown previously that the shape of the approach curves caused by slow IT differs from that typical for finite ET kinetics (e.g., a shallow minimum may appear that is inconsistent with slow ET).[10] No such features can be seen in either Figure 5 or any other approach curve presented below. We thus ascribed the effect of the lipid layer to a decrease in the ET rate.

We obtained several families of SECM current−distance curves for different concentrations of various saturated phospholipids (C-10−C-20) under equilibrium conditions (i.e., at least 40 min after lipid was added to the benzene solution). A typical set is shown in Figure 6 for Ru(CN)$_6$$^{4-}$ species in the

aqueous solution and C-10 lipid in benzene. One can see from the graph that the ET rate decreases monotonically as the lipid concentration increases from 0 μM (curve 2) to 48 μM (curve 6). These show the effect of the growing layer at the interface and represent the combined ET rates at free and covered sites. By fitting the experimental current−distance curves to the theory,[10,13] one can calculate the effective heterogeneous rate constant of the ET reaction that represents an average of those at free and filmed locations. Good agreement between theory (solid lines) and experimental data (symbols) was achieved using a single adjustable parameter $\kappa = k_f a/D$, where a is the tip radius and D = 4 × 10^{-6} cm^2/s is the diffusion coefficient of ZnPor found from steady-state voltammetry at the 7-μm diameter C disk electrode.

Figure 7 presents four dependencies of k_f vs lipid concentration obtained for two different aqueous redox species (Ru(CN)$_6$$^{4-}$

(24) Diamant, H.; Adelman, D. *J. Phys. Chem.* **1996**, *100*, 13732.

(25) (a) Cunnane, V. J.; Schiffrin, D. J.; Fleischman, M.; Geblewicz, G.; Williams, D. *J. Electroanal. Chem.* **1988**, *243*, 455. (b) Kakiuchi, T.; Kondo, T.; Senda, M. *Bull. Chem. Soc. Jpn.* **1990**, *63*, 3270. (c) Kakiuchi, T.; Kondo, T.; Kotani, M.; Senda, M. *Langmuir* **1992**, *8*, 169. (d) Kakiuchi, T.; Kotani, M.; Noguchi, J.; Nakanishi, M.; Senda, M. *J. Colloid Interface Sci.* **1992**, *149*, 279.

and Fe(CN)$_6^{4-}$) and three different lipids (C-10, C-12, and C-20). The two k_f vs [lipid] dependencies shown for Ru(CN)$_6^{4-}$ were obtained with C-10 (filled squares) and C-20 (filled circles). We interpret these results to indicate that the fraction of the interfacial area covered with lipid increases with increasing lipid concentration in benzene and results in a lower ET rate. Thus the curves in Figure 7 can be taken to represent, at least semiquantitatively, an adsorption isotherm for the lipids. At higher concentrations of either lipid (i.e., ≥50 μM) the ET rate between Ru(CN)$_6^{4-}$ and ZnPor becomes immeasurably slow.

The k_f vs [lipid] dependencies for Fe(CN)$_6^{4-}$ (open squares and circles) are different. Although the ET rate decreases markedly with increasing concentration of lipid, it does not vanish at higher concentrations. Instead, it reaches a limiting value at about 50 μM and does not change at higher lipid concentrations. This saturation points to the formation of a complete phospholipid monolayer at the ITIES. In the same concentration range (i.e., [lipid] ≳20 μm), the formation of compact phospholipid monolayers was observed previously at water/nitrobenzene[14c] and water/dichloroethane[14b] interfaces. Apparently, the lipid concentrations required for the formation of a complete monolayer are similar for different organic solvents.

The extent of the blocking effect apparently depends on the driving force for ET (eq 5). When the driving force is small (e.g., $\Delta E°$ ~100 mV for Ru(CN)$_6^{4-}$ and ZnPor$^+$), the formation of any long-chain phospholipid monolayer (i.e., C-10−C-20) results in an ET rate below the lower limit of our SECM measurements (about 5 × 10^{-4} cm/s). This shows that the density of defects in the monolayer is too low to produce detectable feedback current under our experimental conditions. When Ru(CN)$_6^{4-}$ is replaced with Fe(CN)$_6^{4-}$ for which $\Delta E°$ is about 0.5 V larger, ET occurs at a measurable rate via tunneling through the monolayer. If the electrons were transferred through pinholes rather than across the lipid layer, one would expect the ET rate to be independent of the spacer length. In contrast, from the results for Fe(CN)$_6^{4-}$ in Figure 7 for the two lipids at higher concentration, one can see that the longer lipid, C-12 (open squares), inhibits ET more than the C-10 (open circles). An alternative explanation could be that a longer lipid adsorbs more strongly and forms a more compact layer at lower bulk concentrations. If this were so, the C-20 lipid would block the ET reaction between Ru(CN)$_6^{4-}$ and ZnPor$^+$ much more than the C-10. This prediction is in conflict with the data in Figure 7 where the blocking effects produced by the same concentration of C-10 and C-20 are very similar. The assumption that adsorption of longer lipids is stronger would also be at variance with the measured Gibbs adsorption energy values, which are only weakly dependent on the hydrocarbon chain length.[26c] Thus, the lipid adsorption affects differently the ET reactions involving Ru(CN)$_6^{4-}$ and Fe(CN)$_6^{4-}$ because the first process occurs at a measurable rate only at the uncovered portion of the ITIES, while in the second reaction the electron tunneling rate through the monolayer is also significant. At a complete monolayer, the ET through defects does not produce any measurable feedback current.

For the Ru(CN)$_6^{4-}$/ZnPor$^+$ reaction, the dependence of the effective heterogeneous rate constant on the fraction of the ITIES

(26) (a) Girault, H. H.; Schiffrin, D. J. *Biochim. Biophys. Acta* **1986**, *857*, 251. (b) Wandlowski, T.; Marecek, V.; Samec, Z. *J. Electroanal. Chem.* **1988**, *242*, 277. (c) Kakiuchi, T.; Nakanishi, M.; Senda, M. *Bull. Chem. Soc. Jpn.* **1988**, *61*, 1845. (d) Kakiuchi, T.; Nakanishi, M.; Senda, M. *Bull. Chem. Soc. Jpn.* **1989**, *62*, 403.
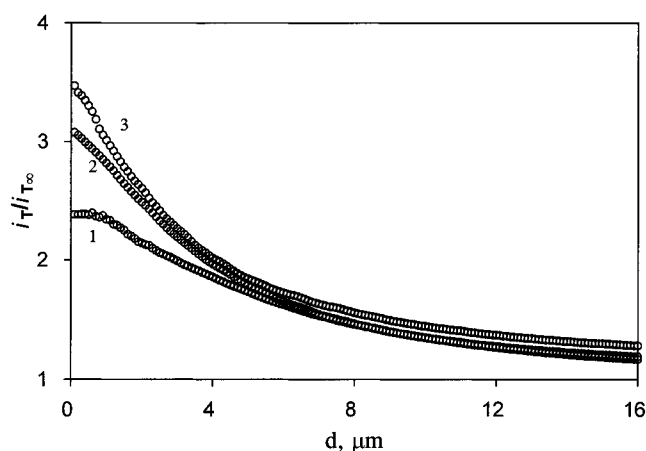

Figure 8. Reversible adsorption of C-10 lipid on the benzene/water interface. The benzene solution initially contained 0.5 mM ZnPor, 0.25 M THAClO$_4$, and 27 μm of C-10 phospholipid (curve 1). The other curves were obtained (2) 5 and (3) 20 min after the organic phase was diluted to decrease the concentration of lipid to 9 μm. Concentrations of ZnPor and THAClO$_4$ were maintained constant. The aqueous solution was 0.1 M NaCl, 0.1 M NaClO$_4$, and 7 mM Na$_4$Fe(CN)$_6$. The 25-μm Pt tip was scanned at 1.0 μm/s.

area covered with lipid (θ) can be evaluated as[27]

$$k_f(\theta) = (1 - \theta)k_f(0) \qquad (8)$$

where $k_f(0)$ is the rate constant at the free ITIES. (This kind of expression cannot be used for a Fe(CN)$_6^{4-}$/ZnPor$^+$ reaction because $k_f(0)$ is too high to be measured. The apparent $k_f(0)$ ~0.03 cm/s in Figure 7 represents only the diffusion limit in our measurements.) The substitution of eq 8 into the Langmuir isotherm

$$B[lipid] = \theta/(1 - \theta) \qquad (9)$$

yields

$$B[lipid] = [k_f(0)/k_f(\theta)] - 1 \qquad (10)$$

The equilibrium adsorption of phospholipids at the ITIES has been studied previously by several groups[14,25,26] and has been shown to follow a Frumkin isotherm

$$B[lipid] = \frac{\theta \exp(-2a\theta)}{1 - \theta} \qquad (11)$$

with a small lateral interaction parameter a and the standard Gibbs energy of adsorption $\Delta G°_{ads} = -RT \ln B$, of about 35−40 kJ/mol.[26c,d] The Langmuir isotherm, which fit our data quite well, represents the limit of the Frumkin isotherm at $a = 0$, in agreement with the previous results. An even better fit could be obtained by using eq 11, but introduces the additional adjustable parameter a. For the Frumkin isotherm, the best fit was obtained for $a = 0.25$ (solid line on Figure 7).

The adsorption of lipids at the ITIES was fully reversible. Curve 1 in Figure 8 represents equilibrium adsorption of 27 μM C-10 at the water/benzene interface. The two other curves in Figure 8 were obtained after the organic phase was diluted with a benzene solution containing the same concentrations of ZnPor and THAClO$_4$ but no lipid, so that the bulk concentration of lipid decreased to 9 μM. Five minutes after dilution (curve 2), one can see a significant decrease in coverage caused by

(27) (a) Amatore, C.; Savéant, J. M.; Tessier, D. *J. Electroanal. Chem.* **1983**, *147*, 39. (b) Forouzan, F.; Bard, A. J.; Mirkin, M. V. *Isr. J. Chem.*, in press.
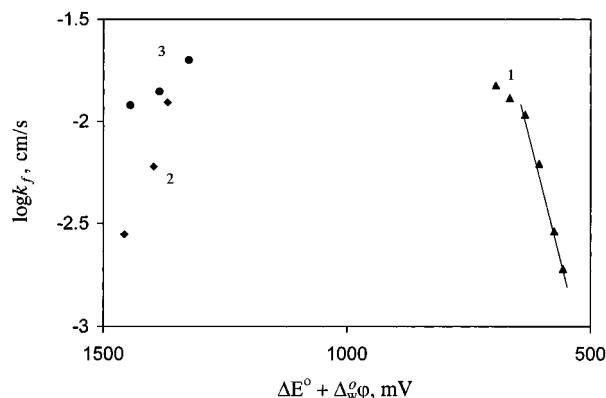
Figure 9. Driving force dependence of the ET rate between $ZnPor^+$ in benzene and various aqueous redox species across a monolayer of C-10 lipid. The organic phase contained 0.25 M $THAClO_4$, 0.5 mM ZnPor, and 100 μM C-10. The aqueous solution contained 7 mM of (1) $Fe(CN)_6^{4-}$, (2) Co(II) sepalchrate, and (3) V^{2+}. For other parameters, see Figure 4.

Figure 10. Tafel plot for ET between $ZnPor^+$ in benzene and aqueous Fe^{2+}. The aqueous solution contained $0.01-2$ M $NaClO_4$, 7 mM Fe^{2+}, and 0.5 M H_2SO_4. For other parameters, see Figure 4. Horizontal dotted line shows the lower limit of measurable rate constant ($\sim 5 \times 10^{-4}$ cm/s).

desorption of lipid from the ITIES. The approach curve obtained 20 min after dilution (curve 3) is very similar to that for equilibrium adsorption of 9 μM C-10. Thus the lipid adsorption on and desorption from the ITIES occur at about the same time scale. The monolayer self-assembled at the ITIES is in dynamic equilibrium with dissolved lipid molecules that allows any pinhole defects to be healed. In contrast, self-assembly on the solid/liquid interface often involves irreversible adsorption and requires high purity of chemicals, complex pretreatment, and preparation protocols to obtain a low defect density molecular monolayer.[4]

Driving Force Dependence of the ET Rate Across a Lipid Monolayer. The potential dependence of the ET rate across the lipid monolayer was measured by the same method discussed above for a free interface. The adsorption of lipid should not affect significantly the potential drop between the water and organic phase, $\Delta_w^o\varphi$, so the driving force for the ET reaction could still be evaluated as the difference between the two half-wave potentials measured with respect to the same aqueous Ag/AgCl reference. As above, a decrease in $[ClO_4^-]_w$ resulted in an increase in driving force for ET. Figure 9 illustrates the driving force dependence of the ET rate across a C-10 lipid monolayer adsorbed on the water/benzene interface for $ZnPor^+$ and three different aqueous redox species. For the $Fe(CN)_6^{4-}$/$ZnPor^+$ reaction, the $(\Delta E^\circ + \Delta_w^o\varphi)$ values obtained by variation of $[ClO_4^-]_w$ were within the range of $570-700$ mV. At lower overpotentials ($\Delta E^\circ + \Delta_w^o\varphi \lesssim 630$ mV), the Tafel plot obtained is linear with a slope of $\alpha = 0.59$. At larger overpotentials, this curve levels off as predicted by Marcus theory[1a]

$$\Delta G^\ddagger = (\lambda_o/4)(1 + \Delta G^\circ/\lambda_o)^2 \qquad (12)$$

where λ_o is the reorganization energy, and ΔG° is given by eq 5. In principle, one can calculate λ_o by fitting the rate dependence in Figure 9 to

$$k_f = k^\circ \exp(-\Delta G^\ddagger/RT) \qquad (13)$$

where the standard rate constant, k°, can either be obtained by extrapolation of the linear portion of the Tafel plot to zero driving force or found as a second adjustable parameter. This result, however, would not be reliable because of a small number of experimental points obtained at higher overpotentials.
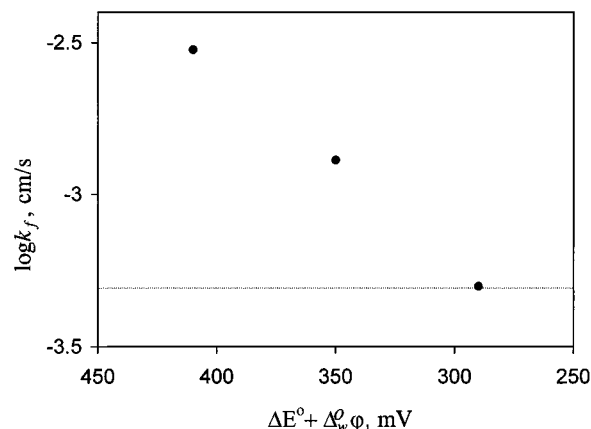
At higher overpotentials (i.e., $\Delta G^\circ > \lambda_o$), eq 12 predicts the existence of an inverted reaction free-energy region, in which the increasing driving force results in a decrease in the ET rate.[1,4c] This effect cannot be observed at metal electrodes, where a continuum of electronic states exists in the metal below the Fermi level. In contrast, the concentrations of redox species in both liquid phases are finite, and one can expect to see the inverted behavior when ΔG° is sufficiently large. Thus the rate constant of the $ZnPor^+/V^{2+}$ reaction decreases significantly over about a 120 mV increase in the driving force (filled circles in Figure 9). An uncertainty in the reliability of these data exists because 0.5 M H_2SO_4 was used as the supporting electrolyte, perhaps causing the protonation of the lipid layer and changing its barrier properties; so another redox couple with a large negative standard potential, $CoSep^{3/2+}$, was used for an additional high driving force control experiment. This couple showed an even more significant decrease in the ET rate with increasing overpotential (diamonds in Figure 9).

One might explain the observed inverted behavior by a double layer effect. Unlike $Ru(CN)_6^{4-}$, $Mo(CN)_8^{4-}$, and $Fe(CN)_6^{4-}$ species, both V^{2+} and $CoSep^{2+}$ are cationic. The higher concentration of ClO_4^- in water corresponds to a more negative $\Delta_w^o\varphi$. This may cause a decrease in interfacial concentrations of cationic redox species and, consequently, a decrease in the ET rate. However, the concentration of supporting electrolyte in the aqueous phase was kept sufficiently high (0.1 M NaCl or 0.5 M H_2SO_4) that double layer effects are unlikely. We have pointed out previously that there is no evidence of strong double-layer effects on the measured rate constants.[13] Further evidence is presented in Figure 10 which shows a Tafel plot for ET between $ZnPor^+$ in benzene and Fe^{2+} in water. Since the aqueous redox mediator here is cationic, the expected double layer effect would be similar to that for the V^{2+} and $CoSep^{2+}$ species. However, no inverted behavior is seen in Figure 10. On the contrary, the Tafel curve is linear, and the transfer coefficient is close to 0.5.

Additional experimental data are needed to obtain a more reliable estimate for the reorganization energy from the potential dependence of the rate constant. It would also be interesting to measure the $k_{1,2}$ and λ_o values for different organic solvents. A comparison of solvent dynamic effects at the metal/solution interface and at the ITIES could provide information about the local environment of the ET reaction at the liquid/liquid interface.

Distance Dependence of ET. The results in Figure 7 suggest that a longer lipid (C-12) produces a stronger blocking effect
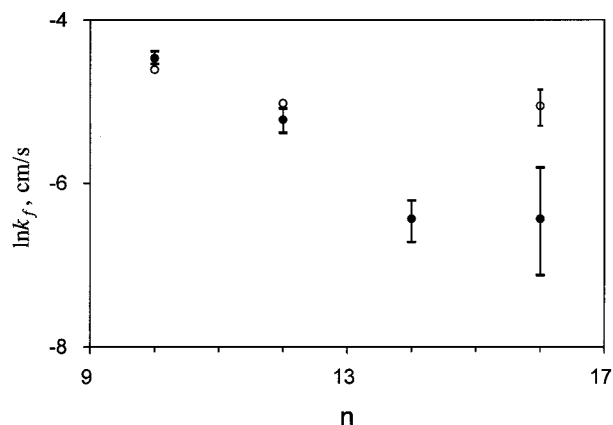
Figure 11. Distance dependence of the ET rate between ZnPor$^+$ and Fe(CN)$_6^{4-}$. The abscissa plots the number of methylene groups in the lipid hydrocarbon chain. The concentration of NaClO$_4$ was 0.1 M, corresponding to a 635 mV driving force for the ET reaction. For other parameters, see Figure 3. The closed and open circles represent results from two independent studies.

on ET between Fe(CN)$_6^{4-}$ and ZnPor$^+$ than a shorter one (C-10). To probe the distance dependence of ET, we obtained data for the ET rate constants for the Fe(CN)$_6^{4-}$/ZnPor$^+$ reaction at the ITIES modified with a monolyer of phospholipids with even longer hydrocarbon chains (C-14, C-16). For any given concentration of perchlorate in the aqueous phase (i.e., a fixed value of $\Delta_w^o\varphi$), the feedback current decreased markedly with an increasing number of methylene groups (n) in a hydrocarbon chain for C-10, C-12, and C-14 lipds (Figure 11). With the C-16 lipid, the results were less reproducible, as shown by the larger scatter and a much larger rate constant measured in an independent study by the same technique.[28] This levelling off in the ln k_f vs n dependence may be caused by the partial penetration of ZnPor$^+$ into the lipid monolayer. The depth of ZnPor$^+$ penetration may be different for the different lipids and, according to the data in Figure 11, is largest for the C-16 lipid. This ZnPor$^+$ penetration prevents any quantitative analysis of the k_f vs n results in terms of a distance dependence of ET. Indeed, even using the C-10−C-14 points, a fit of the ln k_f vs n plot according to the equation[1,4c]

$$k_f(n) = k_f(0) \exp(-\beta n) \qquad (14)$$

yields a β value about one-half of that usually reported.[3,4,29,30] However, penetration depth must be significantly less than the length of the hydrocarbon tail in the lipid molecule. Otherwise, the C-10 monolayer would not decrease the ET rate by several orders of magnitude and the lengthening of the hydrocarbon chain from C-10 to C-14 would not cause k_f to decrease.

(28) Delville, M.-H., Tsionsky, M.; Bard, A. J., in preparation.
(29) Becka, A. N.; Miller, C. J. *J. Phys. Chem.* **1992**, *96*, 2657.
(30) Smalley, J. F.; Feldberg, S. W.; Chidsey, C. E. D.; Linford, M. R.; Newton, M. D.; Liu, Y.-P. *J. Phys. Chem.* **1995**, *99*, 13141.

Conclusions

We have used the SECM to probe the kinetics of heterogeneous ET at the interface between benzene and water and also across a monolayer of lipid. The ET rate at a free interface follows classical (Butler−Volmer) theory. Since no external voltage was applied across the ITIES, these measurements were free of uncompensated *iR* drop and charging current problems typical for conventional techniques. The driving force for ET at the ITIES was shown to be the sum of the standard potential difference and the interfacial potential drop, the additivity of which can be used as a diagnostic criterion to distinguish between ET and IT mechanisms of charge transfer at the liquid/liquid interface.

The effect of adsorption of long-chain saturated phospholipids on the ET rate across the ITIES was used to probe the surface coverage of lipid as a function of time, length of hydrocarbon chain, and concentration of lipid molecules in benzene. In this way, the rate and free energy of adsorption can be measured and an adsorption isotherm established.

The presence of a lipid monolayer on the ITIES significantly decreases the rate of ET, which can be probed over a wide range of overpotentials. This approach, used previously only at solid electrodes through well-organized, defect-free monolayers, is easier to use at the smooth, uniform ITIES than at the solid/liquid interface. The SECM measurements are performed at a nonpolarized interface, so there are no limitations associated with the polarization window of the ITIES. The driving force dependence of the ET rate was probed over a potential range of about 1.5 V. The dependence of ln k_f on driving force (Tafel plot) for ET between Fe(CN)$_6^{4-}$ and ZnPor$^+$ was linear with $\alpha \cong 0.5$ at lower overvoltages and leveled off at more negative $\Delta_w^o\varphi$, as expected from Marcus theory. For much more negative aqueous redox mediators, i.e., V$^{3+/2+}$ and Co(sepalchrate)$^{3+/2+}$, the ET rates decreased, i.e., these were in the Marcus inverted region. This is the first electrochemical observation of inverted behavior for a heterogeneous ET reaction.

The rate of ET decreased with the number of C atoms (n) in the hydrocarbon chain of adsorbed lipid, as predicted by ET theory.[1,4] This suggests that the ET reaction does not occur at defect sites in the lipid monolayer. The dependency of rate with n was interpreted to suggest partial penetration of ZnPor$^+$ into the lipid layer.